Available online at www.sciencedirect.com

ScienceDirect

Procedia CIRP 31 (2015) 465 – 470

www.elsevier.com/locate/procedia

15th CIRP Conference on Modelling of Machining Operations

Experimental and analytical investigation of workpiece thermal load during external cylindrical grinding

Stepan Jermolajev[a]*, Carsten Heinzel[a], Ekkard Brinksmeier[a]

[a]*University of Bremen, IWT, Badgasteiner Str. 3, D-28359 Bremen, Germany*

* Corresponding author. Tel.:+49 (0)421 218-51183; fax: +49 (0)421 218-51102. *E-mail address:* jermolajev@iwt-bremen.de

Abstract

This paper focuses on the correlation between process quantities of an external cylindrical grinding process (heat partition factor ε, specific grinding energy partition u_w transported to the workpiece, specific grinding power P_c'') and resulting surface and subsurface properties of the ground workpiece. In order to identify this correlation, experimental investigations were carried out and the maximum contact zone temperature T_{max} was measured by using a grinding wheel-integrated temperature measurement system. The resulting surface layer properties are linked with the process quantities by means of the regression analysis combined with analytical considerations using the moving heat source theory. The results may contribute to predict resulting surface and subsurface properties of ground workpieces without detailed prior knowledge about thermal and mechanical loads caused by the grinding process.

Peer-review under responsibility of the International Scientific Committee of the "15th Conference on Modelling of Machining Operations

Keywords: Grinding; Energy; Thermal effects; Residual stress; Surface integrity

1. Introduction

In the production of steel parts, a lot of effort is spent to ensure their desired functional behavior at minimum material and production costs. This comes along with continuously increasing requirements on the surface and subsurface properties of machined parts, which are primarily determined by the finishing process [1].

In today's industrial manufacturing, most of the precise functional surfaces are finished by grinding processes. These processes are characterized by a comparatively high specific energy, which may affect the functional surface in diverse ways [2]. For example, process strategies described in [3,4] lead to mechanically induced compressive residual stresses at the workpiece surface. On the opposite, an excessive heat generation during grinding suppresses this mechanical effect and causes thermally induced changes to occur (tensile residual stresses, tempered zones etc.) [5]. Due to very complex interactions that determine the result of a grinding process, the desired workpiece surface and subsurface properties can only be achieved by costly experimental investigations using specific laboratory equipment [2].

This paper presents an analysis of external cylindrical grinding experiments performed at the IWT. Based on the application of multiple linear regression analysis together with assumptions of the moving heat source theory [6,7,8], the specific grinding energy partition u_w transported to the workpiece and the subsequent surface residual stresses σ_{RES} in the direction of the cutting speed (referred to as the tangential surface residual stresses) are calculated and plotted in so-called $P_c'' - \Delta t$ diagram. In combination with the regression model for σ_{RES}, this diagram is sought to identify a reliable grinding process layout at reduced efforts without additional measurement of grinding forces and temperatures. Furthermore, the knowledge of u_w helps to understand the impact of investigated process quantities on resulting surface layer properties.

2. State of the art

A lot of scientific work has been devoted to describe resulting surface and subsurface properties of the ground workpiece as a function of machining parameters and process quantities. This scientific work has so far been focused mainly on the prediction of workpiece thermal damage. It was shown

Peer-review under responsibility of the International Scientific Committee of the "15th Conference on Modelling of Machining Operations

doi:10.1016/j.procir.2015.04.001

that thermally induced changes of workpiece surface and subsurface properties usually occur in connection with significant changes of process quantities, especially contact zone temperatures [2]. This consequently led to the identification of temperature limits, such as the transitional temperature corresponding to the onset of the generation of tensile residual stresses according to [9] or the Ac1-temperature corresponding to austenite formation within the surface layer of the workpiece [7].

Nomenclature

P_c	[W]	Grinding power
P_c''	[W/mm^2]	Specific grinding power
Q_{KSS}	[l/min]	Grinding fluid flow rate
Q_w	[mm^3/s]	Material removal rate
R^2	[-]	Coefficient of determination
T_0	[°C]	Initial workpiece temperature
T_{max}	[°C]	Maximum contact zone temperature
U_d	[-]	Dressing overlap ratio
Δt	[s]	Contact time
α	[mm^2/s]	Workpiece thermal diffusivity
ε	[-]	Heat partition factor
σ_{RES}	[MPa]	Tangential residual stress at the workpiece surface
a_e	[mm]	Depth of cut
b_d	[mm]	Active form roller width
b_w	[mm]	Workpiece width
d_w	[mm]	External workpiece diameter
k	[W/(mm·K)]	Workpiece thermal conductivity
l_g	[mm]	Geometrical contact length
u	[J/mm^3]	Specific grinding energy
u_w	[J/mm^3]	Specific grinding energy partition transported to the workpiece
v_c	[m/s]	Cutting speed
v_{fr}	[mm/min]	Radial feed speed
v_{ft}	[mm/min]	Tangential feed speed

As it was shown in [10,11], resulting surface and subsurface properties after grinding also significantly depend on the contact time Δt that the investigated location at the ground workpiece surface needs to pass through the moving contact zone, which can be seen as a moving heat source:

$$\Delta t = \frac{l_g}{v_{ft}} \tag{1}$$

By varying Δt, the amount of heat dissipated by the workpiece varies as well, which leads to different material modifications. The influence of Δt on the resulting surface and subsurface properties of the ground workpiece can partially be estimated according to time-temperature diagrams and tempering curves known from the conventional heat treatment. However, the reliability of such estimations is limited due to extremely short contact times, i.e. short heat treatment times that are typical for conventional grinding operations [12].

In order to enable a reliable prediction of resulting workpiece surface and subsurface properties after grinding, an experimentally based approach has been proposed by considering the grinding process as short-time heat treatment [13]. Similarly to time-temperature diagrams known from conventional heat treatment, this approach links the resulting surface layer state to the combination of grinding temperatures and corresponding values of Δt. The necessary data basis was acquired during extensive external cylindrical grinding experiments which are described in detail in [13]. The used experimental setup is depicted in Fig. 1. To investigate the influence of varying thermal loads along the workpiece circumference, the depth of cut a_e was continuously increased up to its maximum value during one single workpiece revolution. The transient workpiece temperature field near the ground surface was evaluated by using an infrared temperature measurement system within the grinding tool, detecting the maximum temperature value (referred to as the maximum contact zone temperature T_{max}) during each grinding wheel revolution. Additionally, grinding forces and the grinding power were measured.

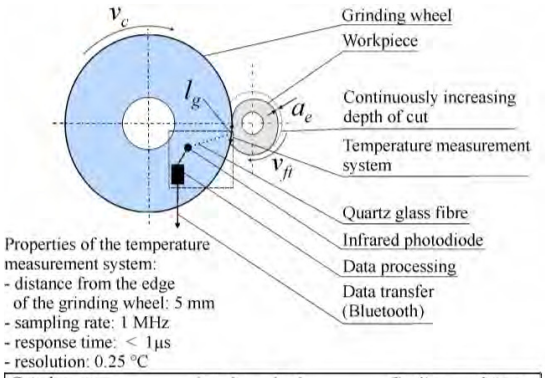

Grinding process:	*Grinding wheel:*	*Cooling conditions:*
External cylindrical plunge grinding	Conventional corundum grinding wheel 400x20x127 A80MM90V	Oil-based grinding fluid
		Free jet nozzle
v_c: 35 - 85 m/s	*Workpiece:*	Q_{KSS}: 20 l/min
a_e: 0 - 0.5 mm	90MnCrV8	*Dressing conditions:*
v_{fr}: 0.5 - 2.0 mm/min	Hardened and tempered to 49+2 HRC	DIA form roller
v_{ft}: 300 - 1800 mm/min	d_W = 100 mm	U_d = 6 (b_d = 0.6 mm)
	b_W = 16 mm, 28 mm	q_d = -0.8

Fig. 1. Experimental setup to measure T_{max} [13].

Ground workpieces were analyzed by using Barkhausen noise measurements, X-ray diffraction, metallographic investigations, and hardness measurements. The resulting workpiece surface and subsurface properties are shown in the developed T_{max} – Δt diagram (Fig. 2). In comparison with [13], this diagram includes additional results from recent experiments performed with high contact zone temperatures and short contact times.

As it can be seen in Fig. 2, specific areas of T_{max} and Δt values can be identified leading to comparable workpiece surface and subsurface properties. For shorter contact times (below 0.40 s) and temperatures above 300 °C, tensile tangential residual stresses σ_{RES} at the workpiece surface were detected. By increasing values of T_{max}, this is followed by the onset of tempered zones (T_{max} above 600 °C) and rehardened zones (T_{max} above 800 °C).

The shown experimental results indicate that the workpiece thermal damage increases with higher values of T_{max} together with low values of Δt. The relation of Δt and T_{max} to the onset of various workpiece material responses to thermal and mechanical load during grinding remains not clear and requires further analysis. In order to contribute to the understanding of this relation, an analysis of the results shown in Fig. 2 by investigating heat partitioning during the grinding process is presented in the following sections.

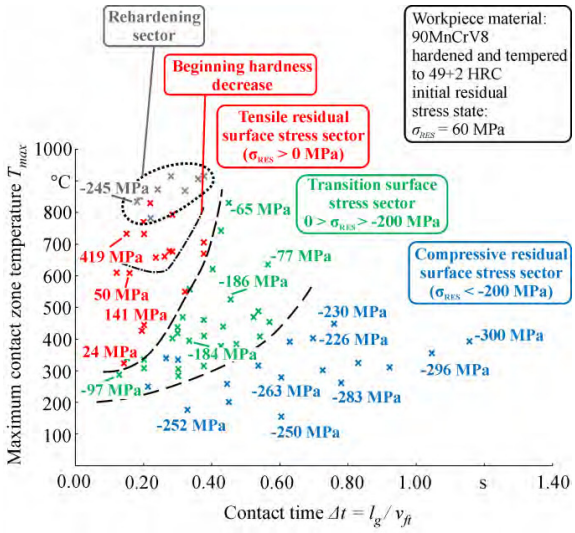

Fig. 2 $T_{max} - \Delta t$ diagram for 90MnCrV8 (after [13]).

3. Research approach and procedures

The objective of this paper is to present a combined experimental and analytical investigation of the external cylindrical grinding process (process layout depicted in Fig. 1). This investigation shall contribute to the identification of possible physically based mechanisms explaining the relation between T_{max}, Δt and σ_{RES}. Further, a tool in the form of a $P_c'' - \Delta t$ diagram combined with approximation of the specific energy partition u_w transported to the workpiece and σ_{RES} applicable in manufacturing will be developed. The sought $P_c'' - \Delta t$ diagram should contain the information about energy partitioning during grinding combined with subsequent tangential residual stresses at the workpiece surface.

The intended analysis is based on experimental results presented in detail in [13]. The experimentally investigated parameters refer to different stages in the causal sequence of a grinding process which is depicted in Fig. 3. Since the general physical relations between machining parameters, process quantities, subsequent internal material load and resulting surface and subsurface properties are so far unknown, a regression analysis was performed to approximate these relations by using adequate regression models. For the purpose of the sought practical tool enabling a more exact definition of thermal limits during grinding, an approximation of σ_{RES} has to be identified together with the specific energy partition u_w transported to the workpiece which corresponds to the heat partition factor ε according to the following equation:

$$u_w = \varepsilon \cdot u = \varepsilon \cdot \frac{P_c}{Q_w} \tag{2}$$

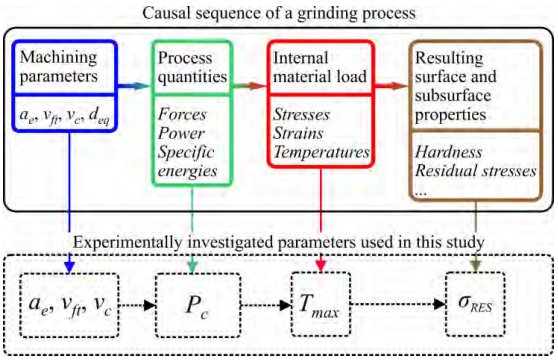

Fig. 3 Experimentally investigated parameters and their relation to the causal sequence of the grinding process (after [14]).

In order to approximate values of ε and u_w by using the variables depicted in Fig. 3, regression models of the third and fourth order would have been necessary. However, such models behave quite unstable especially if the values of input variables are located near the boundaries of investigated intervals. Therefore, ε and u_w will be calculated from T_{max} by considering conclusions of the moving heat source theory [6]. This consequently requires an additional regression model for T_{max} based on known machining parameters and P_c which can be measured by simple means. Apart from ε and u_w, this regression model is also applied to identify the following regression model for σ_{RES}, as seen in the procedure overview depicted in Fig. 4.

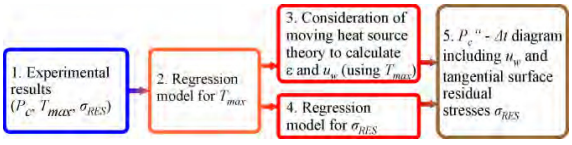

Fig. 4 Procedure to investigate process quantities and resulting surface and subsurface properties of the ground workpieces.

Finally, the calculated values of u_w and predicted values of σ_{RES} were plotted in the $P_c'' - \Delta t$ diagram (last step in Fig. 4). If combined with this diagram, the regression models mentioned above should enable to predict σ_{RES} for the purpose of process optimization by using known machining parameters and process quantities without the measurement of contact zone temperatures and residual stresses. This knowledge is linked with ε and u_w to understand the impact of energy partitioning during grinding on resulting surface and subsurface properties of the workpiece. However, it has to be mentioned that the results of this analysis refer to the process layout depicted in Fig. 1. Changing e.g. dressing and cooling conditions or the grinding wheel specification would require additional experiments by using the temperature measurement system mentioned above.

Based on sudden and unsteady decrease of residual stresses corresponding to the generation of rehardened zones (Fig. 2),

both regression models for T_{max} and σ_{RES} were restricted to temperatures below the threshold of rehardening area (750 °C).

3.1. Identification of the regression models for T_{max} and σ_{RES}

To approximate T_{max} and σ_{RES} by appropriate polynomial regression functions, individual input variables were stepwise added to the model followed by their interactions and higher-order terms. By using the software JMP 7.0, it was possible to check the adequacy of each combination of the input variables according to [15]. This was done in following steps:

- calculating the coefficient of determination R^2
- checking the significance of the whole regression model as well as of the individual variables and their interactions
- comparing the probability distribution of fit errors (residuals) with the normal probability distribution (Shapiro-Wilk test)
- checking the distribution of residuals over time and over predicted values of T_{max} and σ_{RES}
- checking the autocorrelation of residuals (Durbin-Watson test)
- checking the correlation of the individual estimates of regression coefficients

After calculating the value of R^2, a sequence of statistical tests was performed to verify the assumptions of the multiple linear regression analysis [15]. The described sequence was repeated by adding further terms until the value of R^2 reached its maximum.

Since the interactions of input variables were correlated to their individual values, a simple transformation by subtracting the corresponding mean value was applied to avoid a possible deviation of corresponding regressor estimates.

3.2. Calculation of ε and u_w

The calculations of ε and u_w are based on the following analytical expression for T_{max} according to the analytical model from Carslaw and Jaeger [6]:

$$T_{max} - T_0 = \frac{1{,}06 \cdot \varepsilon \cdot P_c}{b_w \cdot k} \cdot \sqrt{\frac{\alpha}{l_g \cdot v_{ft}}} \tag{3}$$

In this equation, a linearly increasing distribution of the heat flux to the workpiece along the contact zone is assumed according to [2,6]. Further, the values of the workpiece material thermal diffusivity α and the workpiece material thermal conductivity k are considered to be constant. Since the value of T_{max} was approximated by using the regression model described above, it is possible to calculate the corresponding value of ε from equation (3) which leads to u_w as a partition of u transported to the workpiece.

4. Results and discussion

4.1. Regression model for T_{max}

In order to find an adequate and simple regression model for T_{max}, the following variables were considered:

- tangential feed speed v_{ft}
- geometrical contact length l_g
- grinding power P_c

This has led to following regression model for T_{max}:

$$T_{max} = 425.79 + 0.24 \cdot (v_{ft} - 921.73) + 102.98 \cdot \\ \cdot (l_g - 4.48) + 0.06 \cdot (v_{ft} - 921.73) \cdot (l_g - 4.48) + \\ +8.48 \cdot (P_c - 1.98)^2 \tag{4}$$

Significant regression coefficients together with boundaries of their 95%-confidence intervals (denoted as lower 95% and upper 95%) and corresponding standard deviations are shown in table 1.

Table 1. Properties of the regression model for T_{max}.

Effect	Coefficient estimate	Lower 95%	Upper 95%	Standard deviation
Intercept in °C	425.79	413.06	438.52	6.31
v_{ft} in mm/min	0.24	0.22	0.26	0.01
l_g in mm	102.98	95.74	110.21	3.59
$l_g \cdot v_{ft}$ in mm²/min	0.06	0.04	0.07	0.01
$P_c \cdot P_c$ in kW²	8.14	0.29	15.99	3.89

The regression model for T_{max} is characterized by its determination coefficient R^2 = 0.97 and error ± 60°C of predicted T_{max}-values.

The form of the regression model presented in equation (4) deviates from purely linear relation between T_{max} and individual regression coefficients. This was expected with regard to non-linear expressions in equation (3). Another fact seen here is that the regression model for T_{max} does not include an individual effect of the cutting speed v_c which was sorted out after performing significance tests described in chapter 3.1. This is most probably due to the effect of P_c^2 which already includes the effect of v_c.

4.2. Resulting plots of ε and u_w over T_{max} and Δt

By means of the regression model for T_{max} and the analytically based expression (3), it is possible to calculate and plot values of ε in the $T_{max} - \Delta t$ diagram. Comparing these values and considering their location in the $T_{max} - \Delta t$ diagram consequently lead to identification of different ε-areas, as seen in Fig. 5. These areas are plotted together with areas of residual stresses shown before (Fig. 2).

The location of ε-areas shown in Fig. 5 indicates that ε is varying with both T_{max} and Δt. According to earlier experimental investigations of energy partitioning during grinding [11], decreasing Δt causes the heat flux to advance towards the ground surface which consequently increases the amount of heat transported to the workpiece. This effect may also be superimposed by the impact of grinding fluid. Large values of l_g combined with low values of v_{ft} corresponding to creep-feed grinding conditions may increase the partition of

grinding heat transported away by the grinding fluid which leads to a significant decrease of ε [2]. In contrast, lower l_g together with increasing v_{ft} corresponding to conventional shallow-cut grinding may cause heat transfer by grinding fluid within the contact zone to be less effective. Consequently, ε increases.

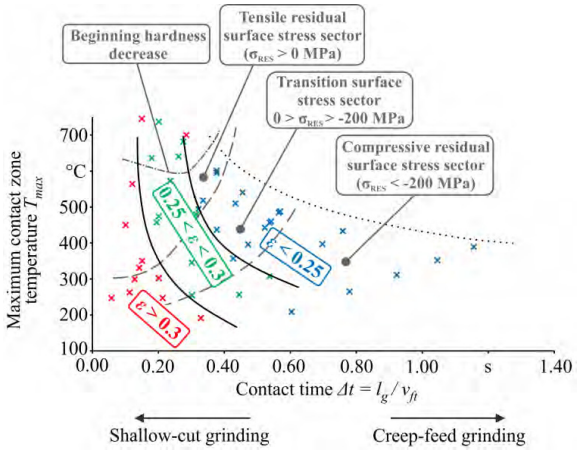

Fig. 5 Areas of ε in $T_{max} - \Delta t$ diagram.

Another fact seen in Fig. 5 is that ε significantly varies with varying T_{max} for a constant Δt. This indicates that the effect of varying Δt is most probably superimposed by an additional physical phenomenon. At lower contact zone temperatures, areas of similar ε expand towards longer contact times. This may be explained by the decreasing amount of heat transported away by grinding fluid which corresponds to a decreasing difference between T_{max} and the initial grinding fluid temperature [16].

After calculating the values of u_w by using the equations (2) and (3), these were plotted over T_{max} and Δt (Fig. 6). Similarly to Fig. 5, three areas of u_w-values were identified. Considering these areas with regard to resulting residual stresses indicates that the same amount of specific grinding energy may cause different material modifications.

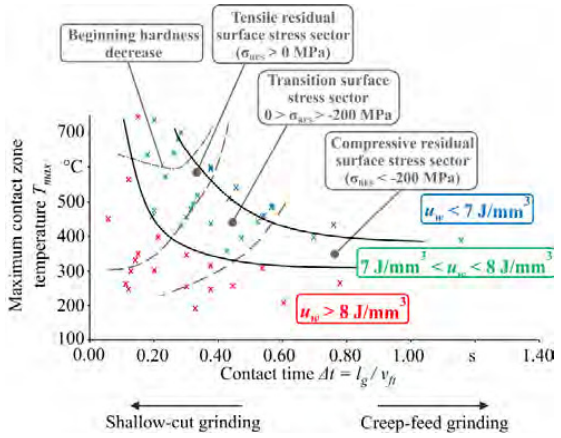

Fig. 6 Areas of u_w in $T_{max} - \Delta t$ diagram.

In combination with short contact times, grinding heat transported to the workpiece cannot be conducted away sufficiently enough. This may quickly lead to excessive thermal load at the ground surface characterized by high contact zone temperatures and consequent significant tensile tangential residual stresses. On the opposite, longer contact times most probably support heat conduction in the normal direction to the ground surface as well as the heat conduction to the workpiece material removed by the advancing grinding wheel. This reduces the resulting contact zone temperature. Thus, contact zone temperatures remain relatively low which favors compressive tangential residual stresses to occur.

4.3. Regression model for σ_{RES}

After performing the regression analysis of σ_{RES} combined with following statistical significance tests according to [15], it was found that σ_{RES} may be reliably predicted by using T_{max} and Δt combined with the specific grinding power P_c'', calculated as:

$$P_c'' = \frac{P_c}{l_g \cdot v_{ft}} \tag{5}$$

Analyzing effects of these variables combined with their interactions consequently led to the following expression:

$$\sigma_{RES} = -372.64 - 536.17 \cdot (\Delta t - 0.38) - \\ -38.44 \cdot \left(P_c'' - 25.98\right) \cdot (\Delta t - 0.38) + 0.55 \cdot \\ \cdot (T_{max} - 433.56) \tag{6}$$

Individual regression coefficients together with their 95%-confidence intervals and standard deviations are presented in table 2.

Table 2. Properties of the regression model for σ_{RES}.

Effect	Coefficient estimate	Lower 95%	Upper 95%	Standard deviation
Intercept in MPa	-372.64	-420.50	-324.78	23.75
Δt in s	-536.17	-611.53	-460.81	37.40
$P_c'' \cdot \Delta t$ in J/mm²	-38.44	-46.83	-30.05	4.16
T_{max} in °C	0.57	0.46	0.69	0.06

The regression model for σ_{RES} is characterized by its determination coefficient R^2 = 0.93 and error ± 80 MPa of predicted σ_{RES}-values. Negative values of regression coefficients corresponding to Δt and $Pc'' \cdot \Delta t$ indicate that the mechanical impact during grinding may be supported by increasing surface-related specific grinding energy at longer contact times, whereby contact zone temperatures should remain as low as possible.

4.4. First approach to plot the $P_c'' - \Delta t$ diagram

In order to draw the sought $P_c'' - \Delta t$ diagram with included values of u_w and σ_{RES}, calculated values of u_w from Fig. 6 were combined with predicted σ_{RES}-values according to equation (6). Consequently, areas of characteristic σ_{RES}-values and

u_w-values were identified (Fig. 7).

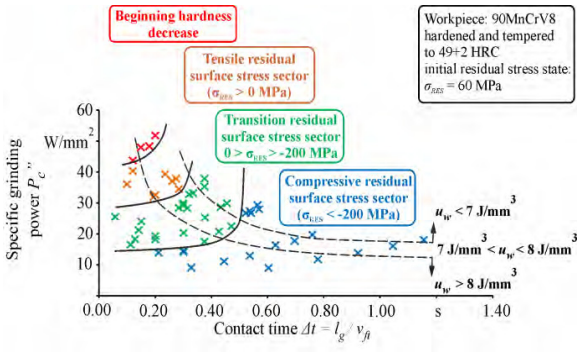

Fig. 7 Areas of σ_{RES} and u_w in $P_c'' - \Delta t$ diagram.

It can be seen that increasing thermal damage of workpiece surface layer corresponds to higher specific grinding power and shorter contact times. On the opposite, longer contact times may reduce u_w by increasing partition of total specific energy transported away by chips and grinding fluid. This consequently reduces the resulting contact zone temperatures and supports the mechanical impact during grinding leading to desired compressive tangential residual stresses.

Together with the regression models for T_{max} and σ_{RES}, the $P_c'' - \Delta t$ diagram shown here may be applied to improve existing process layout by taking into account a more precise consideration of thermal limits on the side of the workpiece made from 90MnCrV8 (49+2 HRC). This enables in-process control of thermal impact during grinding and prediction of subsequent surface and subsurface properties of the workpiece. In addition, it is possible to optimize the specific energy expenditure required to reach desired tangential residual stresses at the workpiece surface. These are predicted only by evaluating P_c'' with regard to corresponding values of Δt without cost-intensive analysis of the workpiece surface layer after grinding.

5. Summary and outlook

Developed regression models together with the $P_c'' - \Delta t$ diagram present an effective tool to predict resulting surface and subsurface properties of the workpiece after grinding. In order to improve the reliability of predicted tangential residual stresses, an additional regression model for T_{max} was specified. This regression model works with a data basis which is available in industrial practice. However, it is necessary to consider the limiting impact of further machining parameters, e. g. dressing and cooling conditions, which may have a significant effect on the resulting adequacy of both regression models. These machining parameters may be included in the proposed regression models by adding additional variables and investigating their impact on T_{max}.

Future investigations will be focused on the described impacts on T_{max} as well as on the comparison of various grinding process kinematics (e. g. external cylindrical grinding, surface grinding) and various grinding wheel specifications. Furthermore, future work will aim at replacing the regression models by physically based models which map process quantities to internal material loads and resulting material modifications. This is expected to increase the extent of validity as well as the scope of application of the presented approach.

6. Acknowledgements

The authors express their sincere thanks to the Deutsche Forschungsgemeinschaft (DFG) for funding the project BR825/58-1 and the subproject F06 within the transregional collaborative research center SFB/TRR 136.

References

[1] Jawahir, I.S., Brinksmeier, E., M'Saoubi, R., Aspinwall, D.K., Outeiro, J.C., Meyer, D., Umbrello, D., Jayal, A.D. Surface Integrity in material removal processes: Recent advances. CIRP Annals – Manufacturing Technology, Volume 60/2, 2011. p. 603-626.

[2] Malkin, S., Guo, Ch. Grinding Technology: Theory and Applications of Machining with Abrasives. 2. Edition, Industrial Press, New York, 2008.

[3] Heinzel, C., Bleil, N. The Use of the Size Effect in Grinding for Work-hardening. CIRP Annals – Manufacturing Technology, Volume 56/1, 2007. p. 327-330.

[4] Denkena, B., Grove, T., Göttsching, T. Grinding with patterned grinding wheels. CIRP Journal of Manufacturing Science and Technology, 2014 (In press, Corrected Proof). DOI: 10.1016/j.cirpj.2014. 10.005.

[5] Aurich, J.C., Linke, B., Hauschild, M., Carrella, M., Kirsch, B. Sustainability of abrasive processes. CIRP Annals – Manufacturing Technology, Volume 62/2, 2013. p. 653-672.

[6] Carslaw, H.S., Jaeger, J.C. Conduction of Heat in Solids. 2. Edition, Oxford University Press, London, 1986.

[7] Malkin, S., Guo, Ch. Thermal analysis of grinding. CIRP Annals - Manufacturing Technology, Volume 56/2, 2007. p. 760-782.

[8] Brinksmeier, E., Aurich, J.C., Govekar, E., Heinzel, C., Hoffmeister, H.W., Klocke, F., Peters, J., Rentsch, R., Stephenson, D.J., Uhlmann, E., Weinert, K., Wittmann, M. Advances in Modelling and Simulation of Grinding Processes. CIRP Annals – Manufacuring Technology, Volume 55/2, 2006. p. 667-696.

[9] Fergani, O., Shao, Y., Lazoglu, I., Liang, S.Y. Temperature Effects on Grinding Residual Stresses. Procedia CIRP, Volume 14, 2004. p. 2-6.

[10] Balart, M.J., Bouzina, A., Edwards, L., Fitzpatrick, M.E. The onset of tensile residual stresses in grinding of hardened steels. Material Science snd Enginnering: A, Volume 367, Issues 1-2, 2004. p. 132-142.

[11] Brinksmeier, E., Minke, E., Wilke, T. Investigations on Surface Layer Impact and Grinding Wheel Performance for Industrial Grind-Hardening Applications. Production Engineering – Research and Development (WGP Annals), Volume 12, Issue 1, 2005. p. 35-40.

[12] Heinzel, C., Sölter, J., Jermolajev, S., Kolkwitz, B., Brinksmeier, E. A versatile method to determine thermal limits in grinding. Procedia CIRP, Volume 13, 2014. p. 131-136.

[13] Jermolajev, S., Brinksmeier, E. A new approach for the prediction of surface and subsurface properties after grinding. Advanced Materials Research, Volume 1018, 2014. p 189-196.

[14] Brinksmeier, E., Klocke, F., Lucca, D.A., Sölter, J., Meyer, D. Process Signatures – A New Approach to Solve the Inverse Surface Integrity Problem in Machining Processes. Procedia CIRP, Volume 13, 2014. p. 429-434.

[15] Montgomery, D.C. Design and Analysis of Experiments. 7. Edition, John Wiley & Sons, Hoboken, 2009.

[16] Brinksmeier, E., Heinzel, C., Wittmann, M. Friction, Cooling and Lubrication in Grinding. CIRP Annals – Manufacturing Technology, Volume 48/2, 1999. p. 581-598.